



THREE-DIMENSIONAL PERTURBATION SOLUTION FOR A DYNAMIC PLANAR CRACK MOVING UNSTEADILY IN A MODEL ELASTIC SOLID

JAMES R. RICE,[†] YEHUDA BEN-ZION[†] and KYUNG-SUK KIM[‡]

[†]Division of Applied Sciences and Department of Earth and Planetary Science, Harvard University, Cambridge, MA 02138, U.S.A.; and [‡]Division of Engineering, Brown University, Providence, RI 02912, U.S.A.

(Received 9 November 1993)

ABSTRACT

A HALF-PLANE CRACK propagates dynamically, nominally in the x direction, along the plane $y = 0$ in an unbounded solid subjected to remote loading equivalent to a static stress intensity factor K^* . The crack front at time t lies along the arc $x = v_0 t + \varepsilon f(z, t)$ where v_0 is a constant velocity, $f(z, t)$ is an arbitrary function, and ε is a small parameter. The crack front speed thus varies along the z axis and its shape deviates from straightness. We address this problem within a model 3D elastodynamic theory involving a single displacement variable u , satisfying a scalar wave equation, and representing tensile opening or shear slippage, with associated tensile or shear stress $\sigma = M \partial u / \partial y$ across planes parallel to the crack, where M is an elastic modulus. The problem is then one of finding a solution to the scalar wave equation satisfying $\sigma = 0$ on $y = 0$ within the rupture. When $\varepsilon = 0$ the solutions for u , σ , dynamic stress intensity factor K and energy release rate G are familiar 2D results. We develop corresponding 3D solutions to first order in ε for arbitrary $f(z, t)$. The solutions are used to address in some elementary cases how a crack front moves unsteadily through regions of locally variable fracture resistance. When a straight crack front approaches a slightly heterogeneous strip, lying parallel to the crack tip along an otherwise homogeneous fracture plane, it may be blocked by asperities after some advancement into the heterogeneous region if it has a relatively small incoming velocity. If, however, the incoming crack velocity is relatively high, the asperities give way and the, now curved, crack front propagates into the bordering homogeneous region. There, the moving crack front recovers a straight configuration through slowly damped space-time oscillations. The oscillatory crack tip motion results from constructive–destructive interferences of stress intensity waves, initiated by encounters of the crack front with asperities, and then propagating along the front. Oscillations in response to a heterogeneity that is spatially periodic in the direction along the crack front decay as $t^{-1/2}$ at large t . The slowness of the decay suggests that the straight crack front configuration may be sensitive to small sustained heterogeneity of the fracture resistance. This is consistent with results of a related analysis (PERRIN and RICE, 1994, in press, *J. Mech. Phys. Solids*) based upon a strictly linearized form of our equations. The persistence of unsteady crack tip motion beyond the immediate region of heterogeneities provides an explanation for high frequency seismic radiation, using a lesser amount of heterogeneity than what might be naively assumed by strict correspondence of all curved and variable velocity portions of a propagating rupture front to asperities. Also, oscillations of crack tip velocity in the presence of sustained small heterogeneities, suggested by features of our 3D results for the model theory, may provide a mechanism for the generation of rough tensile fracture surfaces when the average (macroscopic) propagation speed of the crack is relatively small.

INTRODUCTION

CONSIDER A HALF-PLANE crack propagating in an unbounded solid, nominally in the x direction along the plane $y = 0$ (Fig. 1). The crack front at time t lies along the arc

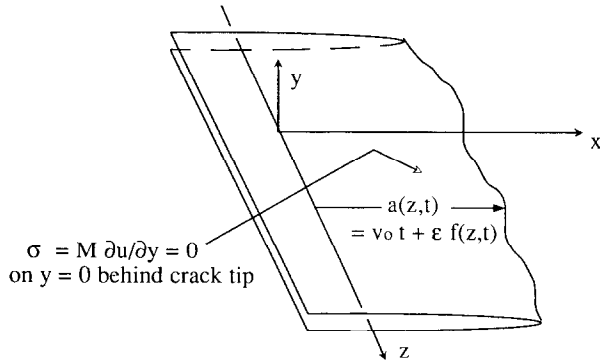


FIG. 1. Half-plane crack in unbounded solid, propagating on plane $y = 0$ with non-straight front.

$x = a(z, t)$ which we assume to have the form $x = v_0 t + \epsilon f(z, t)$, where v_0 is a constant velocity, $f(z, t)$ is an arbitrary function, and ϵ is a small parameter. The crack front speed thus varies along the z axis and its shape deviates from straightness. We address this problem to first-order in ϵ within a *model 3D* elastodynamic theory.

The model theory involves a single displacement variable u , representing tensile opening or shear slippage, and associated tensile or shear stress $\sigma = M \partial u / \partial y$ across planes parallel to the crack, where M is an elastic modulus. The problem is then one of finding a solution to the scalar wave equation

$$c^2 \nabla^2 u = \partial^2 u / \partial t^2 \tag{1}$$

satisfying the boundary condition $\sigma = 0$ on $y = 0$ within the rupture, and meeting remote loading conditions equivalent to a fixed static stress intensity factor K^* . Here $c^2 = M/\rho$ with ρ denoting density. There is no direct connection of the model theory to actual elastodynamics. The latter involves three displacement components and a system of scalar wave equations, coupled by boundary conditions. The model theory results from assuming that a medium occupying volume V , with surface S , on which a loading of intensity q acts, has the Lagrangian (kinetic minus potential energy)

$$L = \int_V \frac{1}{2} \rho \left(\frac{\partial u}{\partial t} \right)^2 dV - \left(\int_V \frac{1}{2} M |\nabla u|^2 dV - \int_S q u dS \right). \tag{2}$$

Hamilton's principle then leads to the scalar wave equation (1) in V and to $M \partial u / \partial n = q$ on S , where n denotes the outer normal direction. Another interpretation of the model 3D theory starts with the actual elastodynamic equations but introduces workless body force constraints in V , and surface traction constraints on S , so that the solid displaces only in a single direction. Then, by an affine transformation of the coordinate axes, the p.d.e. and boundary conditions satisfied by that unconstrained displacement component can be transformed into the model equations assumed here.

An argument concerning the relative order of displacement derivatives in a direction locally parallel to the crack tip, compared to those in direction perpendicular to it, shows that when the crack front arc has a continuously turning tangent, the structure

of the singular field at a 3D crack edge is the same as in a 2D version of the formulation (DMOWKSA and RICE, 1986). Here we are on familiar ground because the 2D version of the model theory involves the same equations as describe states of anti-plane strain in actual elasticity, and the latter has been studied by KOSTROV (1966, 1975) and ESHELBY (1969a, b). Thus, σ on the plane $y = 0$ at distances r ahead of the crack tip satisfies

$$\lim_{r \rightarrow 0} [\sqrt{r}\sigma] = K/\sqrt{2\pi}, \tag{3}$$

where K is the local dynamic stress intensity factor along the crack edge. Also, the relative displacement Δu ($= u_{y=0+} - u_{y=0-}$) of the crack walls at distances r behind the crack tip satisfies

$$\lim_{r \rightarrow 0} [\Delta u/\sqrt{r}] = 2\sqrt{2/\pi}K/M\alpha, \quad \text{with} \quad \alpha = \sqrt{1-v^2/c^2}, \tag{4}$$

where v is the local propagation speed of the crack front and we always assume $v < c$.

Similarly, the relation of the energy release G per unit of new crack area to K and v can be taken from results of the anti-plane theory and is

$$G = K^2/2M\alpha. \tag{5}$$

The fracture criterion is phrased in this work in terms of G . We consider two problems : first, given an arbitrary history of growth of the crack front, $x = a(z, t)$, find the fields $u(x, y, z, t)$ and $\sigma(x, y, z, t)$, and find $K(z, t)$ and $G(z, t)$ along the front. Second, given a distribution $G_{crit}(x, z)$ of the critical value of G over the plane to be fractured, solve for the crack motion $x = a(z, t)$.

We find that the second problem has remarkable stability features. Encounter of the crack front with a periodic row of asperities (isolated regions of higher G_{crit} than the surroundings), lined up in the z direction, is shown to lead to continued, slowly damped, oscillations of $a(z, t)$ and $v(z, t)$ as the crack propagates over the region of uniform G_{crit} lying beyond the asperities. The oscillation amplitude decays only algebraically in time, as $t^{-1/2}$ at large time t , rather than exponentially. In general, a crack with a slightly non-straight front at time t_0 , but which propagates for $t > t_0$ into a region of uniform G_{crit} , will ultimately straighten out. This shows that the straight crack front configuration is stable to isolated perturbations, but the slowness of the recovery of straightness suggests a possible sensitivity to sustained perturbations. Such sensitivity has been demonstrated in a companion paper by PERRIN and RICE (1994) based on what we call the ‘‘strictly linearized’’ version of our formulation. They show that a crack with an initially straight front which enters into a region of sustained small random variations of G_{crit} develops a progressively more disordered front as it propagates, so that the dynamic crack is a configurationally unstable object. Nevertheless, the instability is a gradually developing one for which the variance of the slope of the crack front, and of the deviation of propagation velocity from the mean, increase only with the logarithm of travel distance through the heterogeneous region.

EXACT 2D SOLUTION FOR UNSTEADY CRACK MOTION

Let $x = a(t)$ be the crack growth history in the 2D version of the problem (Fig. 2), in which a straight front propagates in the x direction. We assume that the loadings are such that the static solution of the problem has stress intensity K^* for any position of the crack front, and that all loadings are applied far from the tip compared to distances of interest. Since the 2D version of the model equations are identical to those governing anti-plane strain in actual elastodynamics, we can use the general anti-plane solution for arbitrary crack motion from ESHELBY (1969a, b) to write

$$u(x, y, t) = \sqrt{\frac{2}{\pi}} \frac{K^*}{M} \operatorname{Im} \{ [x - a(\tau) + iy]^{1/2} \}. \tag{6}$$

Here $\tau = \tau(x, y, t)$ is the retarded time at which a signal arriving at position (x, y) at time t was launched at the crack tip (Fig. 2); it satisfies $c^2(t - \tau)^2 = [x - a(\tau)]^2 + y^2$. The analysis applies to an actual finite body prior to the arrival back at the crack tip of waves reflected from boundaries or from another crack tip. The solution very near the tip reduces to

$$u(x, y, t) = \sqrt{\frac{2}{\pi}} \frac{K}{M\alpha} \operatorname{Im} \{ [x - a(t) + i\alpha y]^{1/2} \} + \dots, \tag{7}$$

where α is based on $v(t) \equiv da(t)/dt$ and the dots \dots represent part of the field with higher order spatial variation. The stress intensity factor is

$$K = K(t) = K^* \sqrt{1 - v(t)/c}. \tag{8}$$

Thus we refer to K^* as the “rest” value of K , i.e. the value to which K reverts whenever the crack speed is reduced to zero. The corresponding G is

$$G = G(t) = G^* \sqrt{[1 - v(t)/c]/[1 + v(t)/c]}, \tag{9}$$

where $G^* \equiv (K^*)^2/2M$ is the “rest” value of G .

We derive the 3D solution as a linearized perturbation about the 2D results for a crack moving at a steady speed v_0 , so that $a(t) = v_0t$, and hence for which

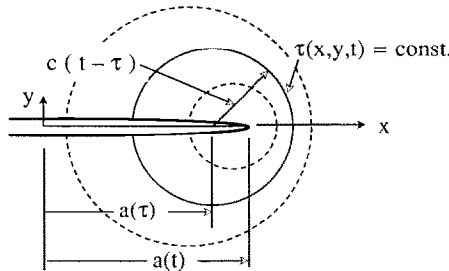


Fig. 2. For the 2D solution with unsteady crack motion: circles of constant travel time shown.

$$K = K_0 \equiv K^* \sqrt{1 - v_0/c}, \quad G = G_0 \equiv G^* \sqrt{[1 - v_0/c]/[1 + v_0/c]}. \quad (10)$$

Then the Eshelby solution (6, 7) above for $u(x, y, t)$ reduces to

$$u = u_0(x, y, t) \equiv \sqrt{\frac{2}{\pi}} \frac{K_0}{M\alpha_0} \operatorname{Im} \{(x - v_0 t + i\alpha_0 y)^{1/2}\} = \sqrt{\frac{2}{\pi}} \frac{K_0}{M\alpha_0} r^{1/2} \sin \frac{\theta}{2}, \quad (11)$$

where

$$\alpha_0 = \sqrt{1 - v_0^2/c^2} \quad (12)$$

and the polar coordinates are understood here and later to denote

$$r e^{i\theta} = x - v_0 t + i\alpha_0 y. \quad (13)$$

This 2D solution is coincident with that of actual elastodynamics for anti-plane strain when we identify M and c with the shear modulus and shear wave speed. The 2D results of FREUND (1972a, b) and FOSSUM and FREUND (1975) for unsteady straight mode I and II cracks are similar in structure to $K(t)$ of (8) with more complex function of $v(t)$ vanishing at the Rayleigh speed.

3D PERTURBATION SOLUTION FOR UNSTEADY CRACK MOTION

We develop the 3D solution for the crack front motion $x = a(z, t) = v_0 t + \varepsilon f(z, t)$ in the form of a first order expansion in ε about the 2D results corresponding to a straight crack ($\varepsilon = 0$) propagating along the x axis with a uniform velocity v_0 . We thus write the displacement field as

$$u(x, y, z, t; \varepsilon) = u_0(x, y, t) + \varepsilon \phi(x, y, z, t) + O(\varepsilon^2), \quad (14)$$

where the first order perturbation term $\phi(x, y, z, t) = [\partial u(x, y, z, t; \varepsilon)/\partial \varepsilon]_{\varepsilon=0}$.

The singular part of the field must be of the 2D character of (6) and (7) above, but now relative to the local direction of crack growth, so that for arbitrary ε

$$u(x, y, z, t; \varepsilon) = \sqrt{\frac{2}{\pi}} \frac{K(z, t; \varepsilon)}{M\alpha(z, t; \varepsilon)} \times \operatorname{Im} \{([x - \{v_0 t + \varepsilon f(z, t)\}] \cos \gamma(z, t; \varepsilon) + i\alpha(z, t; \varepsilon)y)^{1/2}\} + \dots \quad (15)$$

where $\alpha(z, t; \varepsilon) = [1 - v^2(z, t; \varepsilon)/c^2]^{1/2}$, $v(z, t; \varepsilon) = [v_0 + \varepsilon \partial f(z, t)/\partial t] \cos \gamma(z, t; \varepsilon)$, and $\cos \gamma(z, t; \varepsilon) = 1/\{1 + \varepsilon^2 [\partial f(z, t)/\partial z]^2\}^{1/2}$, with γ being the angle between the local normal to the crack front and the x axis. This expression lets us calculate the asymptotic structure as $r \rightarrow 0$ [i.e. as $x \rightarrow a(z, t)$ and $y \rightarrow 0$] of $\phi = [\partial u/\partial \varepsilon]_{\varepsilon=0}$. The result is

$$\lim_{r \rightarrow 0} \{\phi(x, y, z, t) \sqrt{r}\} = \sqrt{\frac{1}{2\pi}} \frac{K_0}{M\alpha_0} f(z, t) \sin(\theta/2). \quad (16)$$

We thus have to find the solution of the scalar wave equation

$$c^2 \nabla^2 \phi = \partial^2 \phi / \partial t^2 \quad (17)$$

satisfying the asymptotic structure (16) and the stress-free boundary condition $\partial\phi/\partial y = 0$ on $y = 0$ when $x < v_0 t$. Note that $\phi = 0$ on $y = 0$ when $x > v_0 t$ by symmetry since displacement u vanishes there. Once ϕ is found, the displacement field u , correct to a first order in ε , is given by (11) and (14).

We begin with the harmonic case $f(z, t) = F(k, \omega) e^{-ikz} e^{i\omega t}$, and seek a solution in the form $\phi(x, y, z, t; k, \omega) = e^{i(\omega t - kz)}$ times a function of the variables $(x - v_0 t)$ and y . We extract an exponential term $\exp[-i\omega v_0(x - v_0 t)/\alpha_0^2 c^2]$ from that function, noting that such will eliminate any first order derivatives in the resulting differential equation for the function, and thus write

$$\phi(x, y, z, t; k, \omega) = \sqrt{\frac{1}{2\pi}} \frac{K_0}{M\alpha_0} F(k, \omega) \exp[i(\omega t - kz)] \cdot \exp[-i\omega v_0(x - v_0 t)/\alpha_0^2 c^2] \psi(x - v_0 t, y; k, \omega), \quad (18)$$

where ψ is a function to be determined. Requiring that ϕ satisfies the wave equation we find that ψ must satisfy

$$\left(\frac{\partial^2}{\partial x^2} + \frac{1}{\alpha_0^2} \frac{\partial^2}{\partial y^2} \right) \psi = \left(\frac{\partial^2}{\partial r^2} + \frac{1}{r} \frac{\partial}{\partial r} + \frac{1}{r^2} \frac{\partial^2}{\partial \theta^2} \right) \psi = q^2 \psi, \quad (19)$$

where

$$q = q(k, \omega) = (1/\alpha_0)(k^2 - \omega^2/\alpha_0^2 c^2)^{1/2} = (1/\alpha_0)(k - \omega/\alpha_0 c)^{1/2} (k + \omega/\alpha_0 c)^{1/2}. \quad (20)$$

To make $q(k, \omega)$ definite in subsequent expressions $(k - \omega/\alpha_0 c)$ is allowed a complex phase angle between 0 and 2π , and $(k + \omega/\alpha_0 c)$ between $-\pi$ and $+\pi$, thus defining branch cuts in the complex ω and k planes. This assures that q behaves as $i\omega/\alpha_0^2 c$ for $|\omega| \gg \alpha_0 c|k|$, and for real k and ω it allows us to write

$$\begin{aligned} q(k, \omega) &= (|k|/\alpha_0)(1 - \omega^2/k^2\alpha_0^2 c^2)^{1/2}, \quad \text{for } \omega^2 < k^2\alpha_0^2 c^2; \\ q(k, \omega) &= (i\omega/\alpha_0^2 c)(1 - k^2\alpha_0^2 c^2/\omega^2)^{1/2}, \quad \text{for } \omega^2 > k^2\alpha_0^2 c^2. \end{aligned} \quad (21)$$

The above expression given for $\omega^2 < k^2\alpha_0^2 c^2$ corresponds to letting k approach the positive real axis through $\text{Im}(k) > 0$ and the negative real axis through $\text{Im}(k) < 0$; the approaches are then to the branch-cut portions of the $\text{Re}(k)$ axis where $|k| > |\omega|/\alpha_0 c$. The expression given for $\omega^2 > k^2\alpha_0^2 c^2$ holds for any direction of approach. The combination $\alpha_0 c$ appears often, and has the following interpretation: suppose that a disturbance is initiated at some point along the crack front. That disturbance spreads out in the medium over a spherical wave front whose radius enlarges at velocity c . The crack front, moving at speed v_0 , intersects that wave front at two points, and those points have velocity components parallel to the crack front (i.e. along the z direction) of $\pm\alpha_0 c$. Hence $\alpha_0 c$ is the speed at which information is transmitted laterally along the moving crack front.

The solution to (18) and (19) satisfying the asymptotic requirement (16) as $r \rightarrow 0$, and meeting the boundary condition $\partial\phi/\partial y = 0$ on the fracture and the symmetry condition, may be taken from an analogous solution by RICE (1985) as

$$\psi(x-v_0t, y; k, \omega) = \frac{1}{\sqrt{r}} \sin\left(\frac{\theta}{2}\right) \{ (1-\beta) \exp [q(k, \omega)r] + \beta \exp [-q(k, \omega)r] \}, \quad (22)$$

where β is an arbitrary constant. Requiring that (22) be bounded at infinity and correspond to only outgoing waves, we set $\beta = 1$. We thus have

$$\phi(x, y, z, t; k, \omega) = \frac{\sin(\theta/2)}{\sqrt{2\pi r}} \frac{K_0}{M\alpha_0} F(k, \omega) \cdot \exp [i(\omega t - kz) - i\omega v_0(x - v_0t)/\alpha_0^2 c^2 - q(k, \omega)r]. \quad (23)$$

Any more general crack perturbation $f(z, t)$ may be represented as a Fourier superposition,

$$f(z, t) = \frac{1}{(2\pi)^2} \int_{-\infty}^{+\infty} \int_{-\infty}^{+\infty} F(k, \omega) \exp [i(\omega t - kz)] dk d\omega \quad (24)$$

such that

$$F(k, \omega) = \int_{-\infty}^{+\infty} \int_{-\infty}^{+\infty} f(z, t) \exp [-i(\omega t - kz)] dz dt \quad (25)$$

is the Fourier transform of $f(z, t)$. Thus the general solution for ϕ is

$$\phi(x, y, z, t) = \frac{\sin(\theta/2)}{\sqrt{2\pi r}} \frac{K_0}{M\alpha_0} \frac{1}{(2\pi)^2} \int_{-\infty}^{+\infty} \int_{-\infty}^{+\infty} F(k, \omega) \cdot \exp [i(\omega t - kz) - i\omega v_0(x - v_0t)/\alpha_0^2 c^2 - q(k, \omega)r] dk d\omega. \quad (26)$$

This solution may be expressed in the space and time domain by evaluating the integrals above on k and ω , after expressing $F(k, \omega)$ as a double integral on space and time of $f(z, t)$, using standard transform methods and analytic function theory. We have done so, but find that a somewhat shorter route is provided by the Cagniard–de Hoop technique (CAGNIARD, 1939, 1962; DE HOOP, 1961; AKI and RICHARDS, 1980), particularly since our problem has a structure similar to a wave problem solved through that technique by BEN-ZION (1989). The derivation is given in Appendix A. The resulting general solution for arbitrary $f(z, t)$, by either route, is

$$\phi(x, y, z, t) = \sqrt{\frac{r}{2\pi}} \frac{K_0 \sin(\theta/2)}{M\alpha_0\pi} \int_{-\infty}^{\infty} \int_{-\infty}^{\infty} \frac{\partial f(z', t')}{\partial t'} \frac{c(t-t') - v_0(x - v_0t)/\alpha_0^2 c}{(z-z')^2 + y^2 + (x - v_0t)^2/\alpha_0^2} \cdot \frac{H[c(t-t') - \sqrt{(z-z')^2 + y^2 + (x - v_0t')^2}]}{\sqrt{c^2(t-t')^2 - (z-z')^2 - y^2 - (x - v_0t')^2}} dt' dz', \quad (27)$$

where $H[]$ is the Heaviside unit step function. Recalling (14), the total displacement field, accurate to first order in ε , is $u(x, y, z, t; \varepsilon) = u_0(x, y, t) + \varepsilon\phi(x, y, z, t)$, with u_0 and ϕ given by (11) and (27) respectively.

3D SOLUTION FOR STRESS INTENSITY FACTOR AND ENERGY RELEASE RATE

When the crack front deviates from straightness, i.e. when $a(z, t) = v_0t + \varepsilon f(z, t)$, the stress intensity factor is perturbed from $K(t)$ of (8). Henceforth it is convenient to replace $\varepsilon f(z, t)$ by $a(z, t) - v_0t$, and $\varepsilon \partial f(z, t)/\partial t$ by $v(z, t) - v_0$, in all expressions. To find the first order perturbation to the stress intensity factor at some location ζ along the z axis, we write the crack front position as a sum of two perturbation terms,

$$a(z, t) = v_0t + [a(\zeta, t) - v_0t] + \{a(z, t) - a(\zeta, t)\}. \tag{28}$$

The square bracket term describes a 2D perturbation, solvable exactly to all orders by (6), (8) and (9), while the curly bracket term corresponds to a 3D perturbation that vanishes at $z = \zeta$ for all t . The stress intensity factor at such points $z = \zeta$, due to small deviation from straightness in other crack front positions, can be found by applying to ϕ of (27) the operator $\lim_{r \rightarrow 0} M\sqrt{2\pi r} \partial/\partial y$. Such a combination of 2D and 3D perturbations of crack location, with the former chosen to make the latter vanish at the point where K is to be evaluated, is the same as developed for elastostatic crack perturbations (RICE, 1985, 1989).

The result, using (3), (8) and (10) and renaming ζ as z in the final expression, is

$$K(z, t) = \sqrt{1 - v_0/c}K^* + [\sqrt{1 - v(z, t)/c}K^* - \sqrt{1 - v_0/c}K^*] + \{\sqrt{1 - v_0/c}K^*I(z, t)\}, \tag{29}$$

where

$$I(z, t) = \frac{1}{2\pi} PV \int_{-\infty}^{\infty} \int_{-\infty}^{t - |z - z'|/\alpha_0 c} \frac{c(t - t')[v(z', t') - v(z, t')]}{(z - z')^2 \sqrt{\alpha_0^2 c^2 (t - t')^2 - (z - z')^2}} dt' dz', \tag{30}$$

with PV denoting the principal value integral and $v(z, t) = \partial a(z, t)/\partial t$ being the local crack velocity. The dependency of the stress intensity factor on crack front shape deviations from straightness is given in the integral $I(z, t)$ above as a functional of velocity differences along the crack tip during the entire history of the crack motion. The part of (29) in square brackets is actually exact for arbitrarily large perturbations of $v(z, t)$, but the curly-bracket part, containing $I(z, t)$, is exact only to first order in the deviation of $v(z, t)$ from v_0 . To develop a better understanding of the 3D history effects, we discuss in Appendix B various alternative forms of $I(z, t)$. One of these, in which α_0 does not appear, but a certain travel time expression does, might possibly be correct to first order in the deviation of the crack front from straightness, i.e. it may not require that $v(z, t)$ remain near v_0 , but only that $v(z, t)$ remain near $v(z', t)$ for all z and z' , although we emphasize that this has not been proven.

The choice of v_0 in the above development is arbitrary as long as it is in the range of "first order difference" from the $v(z, t)$ considered. Using, for example, $v_0 = v(z, t)$ for the curly bracket term of (29) we get

$$K(z, t) = \sqrt{1 - v(z, t)/c}K^*[1 + I(z, t)]. \tag{31a}$$

Alternatively, applying to all terms in (29) a strict linear perturbation about v_0 we get

$$K(z, t) = \sqrt{1 - v_0/c} K^* \left[1 - \frac{1}{2} \frac{v(z, t) - v_0}{c - v_0} + I(z, t) \right]. \tag{31b}$$

In (31a), α_0 of $I(z, t)$ can employ any convenient speed consistent with first order perturbation [e.g. an average in z or t of $v(z, t)$], while in (31b), $\alpha_0 = \sqrt{1 - v_0^2/c^2}$ in agreement with a fully linearized analysis and our previous notation. Expressions (29) and (31a) are written so as to be exact for 2D perturbations of arbitrary size, since in that case $I(z, t) = 0$. We note that the term $K^*[1 + I(z, t)]$ in (31a) has a similar 3D interpretation to that of K^* in 2D problems, i.e. the (now time-dependent) value to which K reduces when the crack speed reduces to zero (if we allow that within our perturbation range), or more generally, the part of $K(z, t)$ which is invariant to instantaneous changes in crack velocity. While a choice between (31b) and (31a) may seem somewhat arbitrary, we note that (31a) incorporates the known exact response to sudden changes in v and, by using methods like in RICE (1985), can also be shown to be exact to first order in the long time limit for a completely arrested crack ($v = 0$). Thus in our numerical simulations, we use (31a) and, in particular, its consequence to follow as (33a) for G .

Examination of the expression for $I(z, t)$ shows that when a segment of the crack front suddenly slows down relative to neighboring locations along the front, a reduction in K radiates outward from that segment at speed $\alpha_0 c$. Similarly, when a segment speeds up, an increase of K is radiated. Such elementary slow-down and speed-up events occur when a crack front encounters regions of higher or lower fracture resistance. Typically, when a localized region of that type is passed by the crack tip, a slow-down is followed by a speed-up, or conversely, so that pairs of K waves are radiated. As will be seen in subsequent examples, the constructive and destructive interferences which result when such waves meet one another, after the crack has propagated beyond the local heterogeneities of fracture resistance which launched them, can lead to continuing fluctuations of the crack front shape and propagation velocity even when the front is moving through material of locally uniform fracture resistance.

The fracture criterion adopted in this work is given by the requirement that

$$G(z, t) = G_{\text{crit}}(x, z) \tag{32}$$

at points $x = a(z, t)$ along the rupture front where $v(z, t) > 0$. Here $G(z, t)$ is the energy release rate per unit of new crack area and the critical energy release rate, $G_{\text{crit}}(x, z)$, is regarded as a material property. This criterion is well known to be consistent as a limiting case with elastodynamically analysed cohesive zone tensile crack models, or slip-weakening shear crack models, when the zone of strength degradation is small compared to other relevant dimensions (e.g. RICE, 1980). Using the energy release rate given in (5), and $K(z, t)$ of (31a), we find to the accuracy considered,

$$G(z, t) = \sqrt{\frac{1 - v(z, t)/c}{1 + v(z, t)/c}} G^* [1 + I(z, t)]^2, \tag{33a}$$

where $G^* = (K^*)^2/2M$ is the rest energy release rate supplied to a straight crack front.

The strictly linearized form of this expression, most conveniently given for $\sqrt{G(z, t)}$, is

$$\sqrt{G(z, t)} = \sqrt{G_0} \left\{ 1 - \frac{c[v(z, t) - v_0]}{2(c^2 - v_0^2)} + I(z, t) \right\}, \tag{33b}$$

where G_0 is given by (10).

From (32) and (33a), the space and time varying motion of the (massless, potentially non-straight) crack front is governed by

$$v(z, t) = \begin{cases} c \frac{1 - \Lambda^2(z, t)}{1 + \Lambda^2(z, t)} & \text{if } \Lambda(z, t) < 1 \\ 0 & \text{if } \Lambda(z, t) \geq 1, \end{cases} \tag{34}$$

where $\Lambda(z, t) = G_{\text{crit}}[a(z, t), z] / \{ [1 + I(z, t)]^2 G^* \}$ and, recalling (30), $I(z, t)$ is a functional of the prior history of $v(z, t)$.

FOURIER REPRESENTATION OF RESULTS

For purposes of numerical analysis of spontaneous crack growth, and for some stability studies, it is convenient to recast the results above in terms of Fourier components, in z , of $a(z, t)$. We rewrite (see Appendix B) the double integral $I(z, t)$ of (30) as

$$I(z, t) = \frac{1}{2\pi} \int_{-\infty}^t \int_{z - \alpha_0 c(t-t')}^{z + \alpha_0 c(t-t')} \frac{c(t-t')[v(z', t') - v(z, t')]}{(z-z')^2 \sqrt{\alpha_0^2 c^2 (t-t')^2 - (z-z')^2}} dz' dt', \tag{35}$$

where the principal value of the integral is assumed implicitly. Using in (35) the variable substitution $z' = z + \alpha_0 c(t-t') \sin \theta$ gives

$$I(z, t) = \frac{1}{2\pi\alpha_0} \int_{-\infty}^t \frac{1}{\alpha_0 c(t-t')} \int_{-\pi/2}^{\pi/2} \frac{v[z + \alpha_0 c(t-t') \sin \theta, t'] - v(z, t')}{\sin^2 \theta} d\theta dt'. \tag{36}$$

We use for $a(z, t)$ and $v(z, t)$ the (periodic over some large length λ) Fourier representations

$$a(z, t) = \sum_{n=-N}^N A_n(t) e^{i2\pi n z/\lambda} \quad \text{and} \quad v(z, t) = \sum_{n=-N}^N \dot{A}_n(t) e^{i2\pi n z/\lambda}, \tag{37}$$

where N is any convenient truncation of the series for the accuracy required, and the over-dot denotes a derivative with respect to time. Consistent with a first order perturbation, one requires $nA_n/\lambda \ll 1$ and $\dot{A}_n/(c-v_0) \ll 1$, and we assume $A_n(-\infty) = 0$ for $n \neq 0$. We thus obtain for the integral $I(z, t)$ the series

$$I(z, t) = \sum_{n=-N}^N I_n(t) e^{i2\pi n z/\lambda}, \tag{38}$$

where the coefficients are obtained from (36) and (37) as

$$I_n(t) = \frac{1}{2\pi\alpha_0} \int_{-\infty}^t \frac{\dot{A}_n(t')}{\alpha_0 c(t-t')} \int_{-\pi/2}^{\pi/2} \frac{\exp(i\beta \sin \theta) - 1}{\sin^2 \theta} d\theta dt', \quad \beta = 2\pi n\alpha_0 c(t-t')/\lambda. \tag{39}$$

Denoting the integral with respect to θ above as $Q(\beta)$, we note that $Q''(\beta) = -\pi J_0(\beta)$, where J_0 is the Bessel function of order zero. Integrating twice with respect to β using the conditions $Q(0) = Q'(0) = 0$ and the relations between the Bessel functions $J_0(\beta)$ and $J_1(\beta)$, we find

$$I_n(t) = -\frac{\pi n}{\alpha_0 \lambda} \int_{-\infty}^t \dot{A}_n(t') F[2\pi n\alpha_0 c(t-t')/\lambda] dt', \tag{40}$$

where the function $F[2\pi n\alpha_0 c(t-t')/\lambda]$, satisfying $F(0) = 0$ and $F(\infty) = 1$, is defined by

$$F(q) = \int_0^q \frac{J_1(p)}{p} dp = \int_0^q J_0(p) dp - J_1(q). \tag{41}$$

The Fourier decompositions (37) and (38), and (40) for $I_n(t)$, allow rapid numerical conversions between the crack front evolution $a(z, t)$ and the histories of $I(z, t)$ and $G(z, t)$.

INTERPRETATION OF THE SOLUTION FOR A PLATE OF FINITE THICKNESS

Thus far we have assumed that the crack propagates as a half-plane crack in an unbounded solid. Suppose instead that the solid is a plate with finite thickness H in the z direction. Assuming that the lateral surfaces of the plate are free from loading, the boundary condition to be satisfied on those surfaces is $\partial u/\partial z = 0$; this follows from applying Hamilton's principle to (2). The solution given here for the infinitely thick solid will meet that condition if we define $a(z, t)$ on the range of the z axis laying outside the plate such that $a(z, t)$ has mirror symmetry about the two values of z corresponding to the plate surfaces. This operation extends $a(z, t)$ to the entire z axis as a periodic function of period $2H$; such may be represented by a Fourier series like in (37) with $\lambda = 2H$, which is, by the mirror symmetry, equivalent to a cosine series expansion in z over the domain of the plate.

MODAL ANALYSIS OF RECOVERY OF THE STRAIGHT CRACK FRONT FROM A PERTURBATION

We now show analytically, using a slightly simplified framework, that a crack front in a homogeneous region bounding a heterogeneous strip approaches a straight configuration through oscillations in time and space that damp only algebraically in time, as $1/\sqrt{t}$, at large time. The fully linearized measure $\sqrt{G(z, t)}$ of energy release

rate is given in (33b). Putting in (33b) the Fourier representations of $v(z, t)$ and $I(z, t)$ [see (37), (38) and (40)] we have

$$\sqrt{G(z, t)} = \sqrt{G_0} \left\{ 1 + \frac{cv_0}{2(c^2 - v_0^2)} - \sum_{n=-N}^N \left[\frac{c}{2(c^2 - v_0^2)} \dot{A}_n(t) + \frac{\pi n}{\alpha_0 \lambda} \int_{-\infty}^t \dot{A}_n(t') F(\beta) dt' \right] e^{i2\pi n z / \lambda} \right\}, \quad (42)$$

where $\beta = 2\pi n \alpha_0 c(t - t') / \lambda$.

The material property $\sqrt{G_{crit}(x, z)}$, assumed to be only slightly inhomogeneous for consistency with a first-order perturbation, can be written as a Fourier series

$$\sqrt{G_{crit}(x, z)} = \sum_{n=-N}^N g_n(x) e^{i2\pi n z / \lambda}. \quad (43)$$

In using the fracture criterion (32), we may approximate x as $v_0 t$, as is consistent with a strictly linearized analysis in perturbation amplitude. Thus, the equation governing the crack tip motion is given by the requirement $\sqrt{G(z, t)} = \sqrt{G_{crit}(v_0 t, z)}$. Using (42) and (43), we then get for $n = 0$

$$\sqrt{G_0} \left\{ 1 + \frac{c[v_0 - \dot{A}_0(t)]}{2(c^2 - v_0^2)} \right\} = g_0(v_0 t), \quad (44a)$$

and for $n \neq 0$

$$\sqrt{G_0} \left\{ \frac{c}{2(c^2 - v_0^2)} \dot{A}_n(t) + \frac{\pi n}{\alpha_0 \lambda} \int_{-\infty}^t \dot{A}_n(t') F[2\pi n \alpha_0 c(t - t') / \lambda] dt' \right\} = -g_n(v_0 t). \quad (44b)$$

Using in (44b) the substitution $\tau = 2\pi |n| \alpha_0 c t / \lambda$ we have

$$(1/D_n) \left[\dot{A}_n(\tau) + \int_{-\infty}^{\tau} \dot{A}_n(\tau') F(\tau - \tau') d\tau' \right] = -g_n(\tau), \quad (45)$$

where $1/D_n = \sqrt{G_0} \pi |n| / \alpha_0 \lambda$, and where, in this equation and henceforth in this section, the over-dot denotes a derivative with respect to the argument τ or τ' and $g_n(\tau)$ denotes what was called $g_n(v_0 t)$ evaluated with $v_0 t = v_0 \lambda \tau / 2\pi |n| \alpha_0 c$. Applying the Laplace transform to both sides of (45) and setting $\dot{A}_n(\tau) = B_n(\tau)$, we find

$$B_n(s)[1 + F(s)] = -D_n g_n(s), \quad (46)$$

where $B_n(s) = L[B_n(t)]$, etc. and $L[]$ denotes the Laplace transform of a function. The function $F(s)$ is given from (41) and expressions of ABRAMOWITZ and STEGUN (1972) as

$$F(s) = (1/s)L[J_0(\tau)] - L[J_1(\tau)] = -1 + \sqrt{s^2 + 1}/s, \quad (47)$$

so that (46) gives

$$B_n(s) = -D_n s g_n(s) / \sqrt{s^2 + 1}. \tag{48}$$

Applying an inverse Laplace transform to (48) we obtain the modal velocity response to a toughness heterogeneity as

$$B_n(\tau) = \dot{A}_n(\tau) = -D_n \int_0^\tau \dot{g}_n(\tau') J_0(\tau - \tau') d\tau'. \tag{49}$$

For present purposes it suffices to consider now a simple case of a finite-width strip, having a single $m \neq 0$ Fourier component of heterogeneity, embedded in an otherwise homogeneous medium. Specifically, we assume that besides g_0 , which is constant at $\sqrt{G_0}$, only $g_m(\tau)$ and $g_{-m}(\tau)$ are non-zero (they are complex conjugates of one another). We write

$$g_m(\tau) = g_{-m}(\tau) = (p\sqrt{G_0}/2)[H(\tau - \tau_1) - H(\tau - \tau_2)], \tag{50}$$

where H is the Heaviside unit step function and p is the (small) amplitude of the perturbation in $\sqrt{G_{crit}(x, z)}$ in the heterogeneous strip encountered between the (dimensionless) times τ_1 and τ_2 . Thus the fracture resistance in the strip is heterogeneous in the z direction (in a single Fourier mode m) but homogeneous with respect to x , apart from discontinuities in resistance upon entering and leaving the strip. Putting (50) into (49) we get

$$\dot{A}_m(\tau) = \dot{A}_{-m}(\tau) = -(p\sqrt{G_0}/2)D_m[J_0(\tau - \tau_1)H(\tau - \tau_1) - J_0(\tau - \tau_2)H(\tau - \tau_2)]. \tag{51}$$

That is, writing $\hat{\lambda}$ for $\lambda/|m|$, the result is that the response to

$$\sqrt{G_{crit}(x, z)} = \sqrt{G_0}[1 + p \cos(2\pi z/\hat{\lambda})] \tag{52}$$

for x within the strip, with $\sqrt{G_{crit}(x, z)} = \sqrt{G_0}$ for x outside it, is that the propagation velocity is

$$v(z, t) = v_0 - [2\alpha_0^2 c p \cos(2\pi z/\hat{\lambda})][J_0(\tau - \tau_1)H(\tau - \tau_1) - J_0(\tau - \tau_2)H(\tau - \tau_2)] \tag{53}$$

to first order in p , where now $\tau = 2\pi\alpha_0 ct/\hat{\lambda}$.

Since the Bessel function describes decaying oscillations we see from (53) that when a straight crack enters a heterogeneous region its motion is modulated by a set of decaying oscillations; when the crack leaves the heterogeneous strip a second set is activated with an opposite sign. Using the asymptotic expansion $J_0(\tau) \approx \sqrt{2/\pi\tau} \cos(\tau - \pi/4)$, valid for $\tau \gg 1$, we see that for $\tau \gg \tau_2$ and for $\tau_2 - \tau_1$ not equal to a multiple of 2π (i.e. the time to transit the strip is not a multiple of the time for a crack front wave to traverse the period $\hat{\lambda}$), the velocity perturbation is proportional to the damped oscillatory function $\cos(\tau + \text{constant})/\sqrt{\tau}$. The very slow damping of this oscillatory motion raises the possibility that indefinitely continuing small random fluctuations in the critical energy release rate may lead to a response in which the crack front becomes increasingly more disordered with propagation length or time. As noted in the Introduction, this has been proven based on the structure of our strictly linearized equations by PERRIN and RICE (1994).

NUMERICAL PROCEDURE

In this section the previous results are used to simulate the dynamic growth of a crack along a plane having a non-uniform distribution of critical energy release rate. The plane of the crack is characterized by a homogeneous "background" critical energy release rate, $G_{\text{crit}0}$, from which there are local perturbations where $G_{\text{crit}}(x, z) \neq G_{\text{crit}0}$. The line $x = 0$ is located so as to be a lower bound (not necessarily the upper-most lower bound) of the heterogeneous (half-plane) region, so that $G_{\text{crit}}(x < 0, z) = G_{\text{crit}0}$ and $v(x < 0, z) = v_0$, i.e. the crack front in the region $x < 0$ is straight (see, e.g. Fig. 3). The (dimensionless) parameters of the problem are v_0/c and $G_{\text{crit}}(x, z)/G_{\text{crit}0}$ [or the uniquely related pair $G_{\text{crit}0}/G^*$ and $G_{\text{crit}}(x, z)/G^*$]. Space is discretized into $2N \cdot M$ cells of size Δz , Δx and time is discretized into steps $\Delta t \leq \lambda/Nc$, where λ is the fundamental periodic length of the problem and $2N$ is the number of uniformly spaced sampling points used in the Fast Fourier Transform (FFT) of the space variable z .

As stated earlier, the developments of this work are based on first order perturbation theory. FARES (1989) examined the limitations of first-order-analysis for a quasi-static problem analogous to that of the present work. Comparing Boundary Element Method calculations to results of RICE (1985) based on a linear perturbation solution, FARES (1989) found that for a crack front shape in the form of a cosine wave, the first order results for the stress intensity factor are within 7% of those given by the Boundary Element Method calculations, when the ratio of amplitude to wavelength of the cosine wave does not exceed about 0.1. For periodic circular asperities, separated by two asperity-diameter, FARES (1989) found that the first-order quasi-static theory is valid for cases having ratios of critical stress intensity factors of asperity and non-asperity regions that do not exceed approximately two [the corresponding ratio for

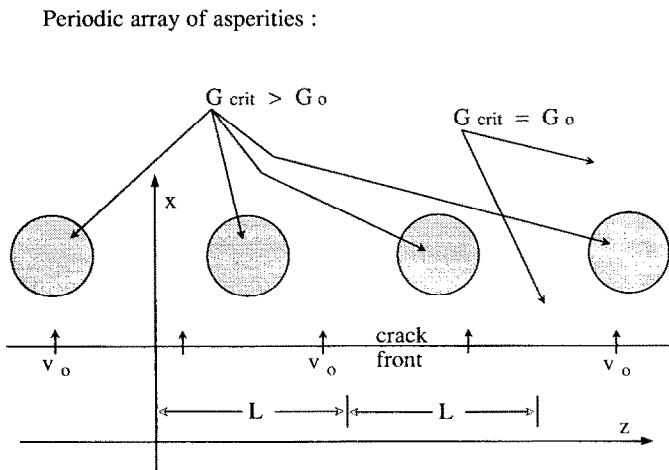


FIG. 3. A crack with an initially straight front, about to encounter a periodic row of circular asperities of higher fracture toughness. The incoming crack velocity is v_0 and the critical fracture energy G_{crit} outside the asperities is constant at G_0 ; G_{crit} is higher on the asperities.

critical energy release rates is four; see GAO and RICE (1989) for more discussion of the validity of first-order quasi-static theory]. The cases examined below satisfy the criteria of FARES (1989) for validity of first order perturbation quasi-static analysis, although those criteria do not, of course, fully guarantee the validity of the dynamic calculations done here.

Our simulations begin with a straight crack propagating with a uniform velocity v_0 in the region $x < 0$. The calculation of space and time varying dynamic crack propagation in the heterogeneous region $x > 0$ (correct to first order) is done using the following procedure.

(1) Having crack front positions and velocities at a general (discrete) time step $m\Delta t$, use the FFT procedure to calculate from current velocities $v(z, m\Delta t)$ the Fourier coefficients $\dot{A}_n(m\Delta t)$ of (37); verify that first order perturbation conditions $\dot{A}_n/v_0 \ll 1$, $n\dot{A}_n\Delta t/\lambda \ll 1$ are satisfied.

(2) Calculate local crack front velocities for the next time increment as follows:

(2.1) use (40) and history of \dot{A}_n to calculate the coefficients $I_n(m\Delta t)$;

(2.2) use FFT to invert $I_n(m\Delta t)$ to $I(z, m\Delta t)$;

(2.3) use (34) and current crack front positions to calculate velocities $v(z, (m+1)\Delta t)$ during the next time step.

(3) Calculate the local crack front positions at the end of the next time step as

$$a(z, (m+1)\Delta t) = a(z, m\Delta t) + v(z, (m+1)\Delta t)\Delta t.$$

(4) Write output; check exit criteria (location of crack front or violation of first order conditions); increase time index m by 1, go to step (1).

We note that the above procedure employs the simplification that the fields are constant within (and hence change discontinuously between) the discrete time steps.

ROW OF CIRCULAR ASPERITIES

As a basic configuration for calculated examples we consider the case studied quasi-statically by GAO and RICE (1989) and FARES (1989). Figure 3 shows a periodic array of circular asperities with radius R and center-to-center spacing L . Following the conditions of FARES (1989) for the validity of quasi-static first-order-analysis, we choose $R/L = 0.1$ and $G_{\text{crit a}}/G_{\text{crit 0}} \leq 4$, where $G_{\text{crit a}}$ and $G_{\text{crit 0}}$ denote the critical energy release rates in the asperity and non-asperity regions, respectively.

Figure 4 shows crack front profiles in the region $x > 0$ at successive times, calculated for the case $v_0/c = 0.3$ and $G_{\text{crit a}}/G_{\text{crit 0}} = 4$ for both left and right asperities in a fundamental wavelength $\lambda = 2L$. The computations are done using $M = 2N = 256$ and $\Delta t = \lambda_{\text{Ny}}/5c$ where $\lambda_{\text{Ny}} = \lambda/N$ is the Nyquist wavelength of the spatial Fourier decomposition. For the ratios v_0/c and $G_{\text{crit a}}/G_{\text{crit 0}}$ of Fig. 4, the asperities block the crack advancement after it penetrates into the inter-asperity $G_{\text{crit 0}}$ region a maximum distance of about $0.2L$. Figure 5 shows results for $v_0/c = 0.3$, $G_{\text{crit a}}(\text{left})/G_{\text{crit 0}} = 4$ and $G_{\text{crit a}}(\text{right})/G_{\text{crit 0}} = 3$, where $G_{\text{crit a}}(\text{left})$ and $G_{\text{crit a}}(\text{right})$ denote, respectively, the critical energy release rates of the left and right asperities in a fundamental

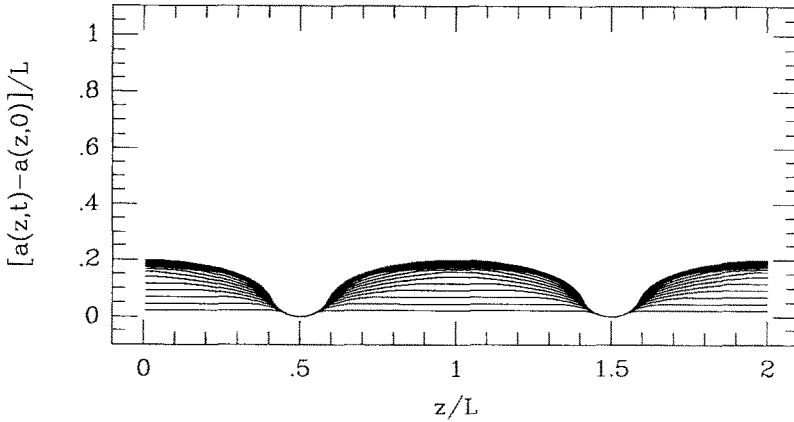


FIG. 4. Positions $a(z, t)$ versus z at successive times, separated by constant intervals, for a crack at incoming speed $v_0 = 0.3c$ hitting an infinite row of asperities with $G_{crit} = 4G_0$. The crack is trapped by the asperities.

wavelength. For this case, the energy release rate induced by the shape deviation due to the inter-asperity crack penetration reaches the value $G_{crit a}$ (right), thus breaking the weaker right asperity toward the end of the computation time. Figure 6 shows calculations for $G_{crit a}$ (right)/ $G_{crit 0} = 2$ and the other parameters as in Figs. 3 and 4. Here, the right asperity breaks when the inter-asperity penetration distance is about $0.18L$. Then, after some further crack front motion, the left asperity gives way too and the crack propagates into the homogeneous $G_{crit 0}$ region where it approaches a straight configuration through damped oscillatory motion.

The mechanism by which the crack front straightens itself with oscillations of

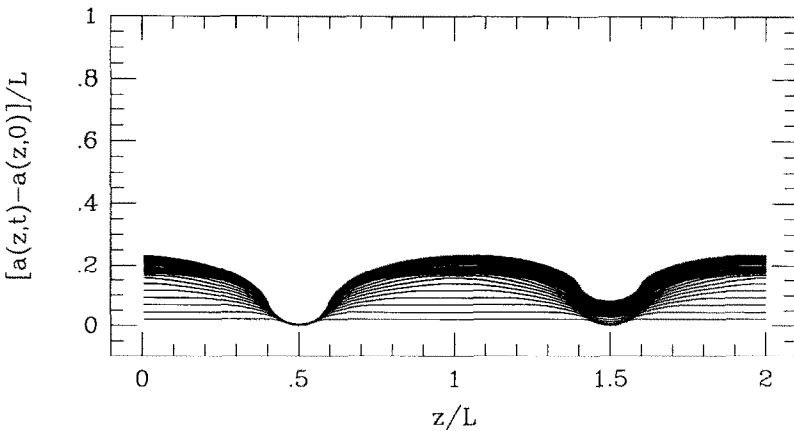


FIG. 5. Positions $a(z, t)$ versus z at successive times, separated by constant intervals, for a crack at incoming speed $v_0 = 0.3c$ hitting an infinite row of asperities with alternating toughnesses, $G_{crit} = 4G_0$ (as on left) and $G_{crit} = 3G_0$ (as on right). The crack is again trapped but now penetrates slightly into the less tough asperities.

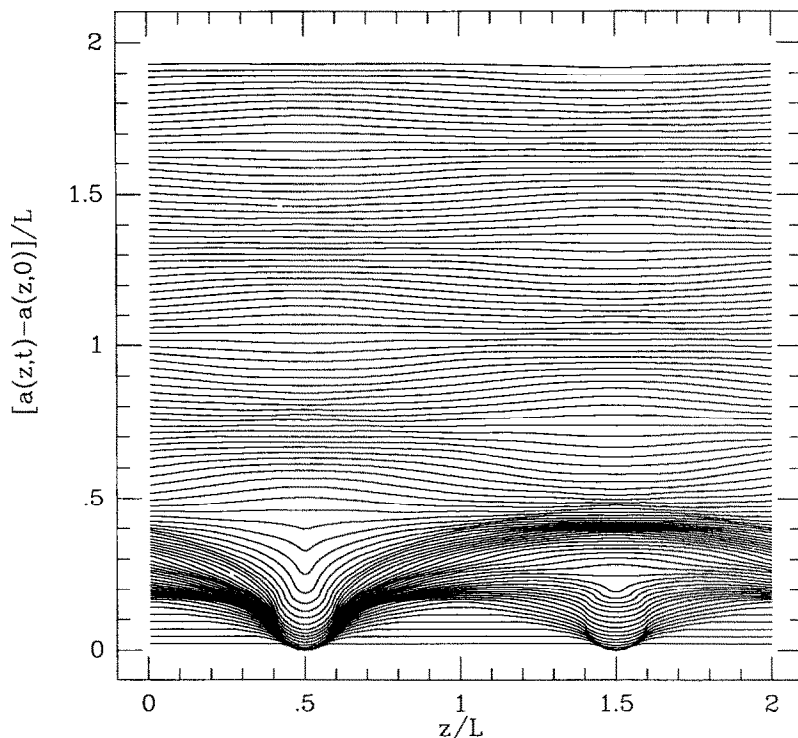


FIG. 6. Positions $a(z, t)$ versus z at successive times, separated by constant intervals, for a crack at incoming speed $v_0 = 0.3c$ hitting an infinite row of asperities with alternating toughnesses, $G_{crit} = 4G_0$ (as on left) and $G_{crit} = 2G_0$ (as on right). The crack nearly arrests but is able to propagate through the less tough asperities, after which it is able to further load the tougher asperities and break them too. Note the pronounced oscillations of the crack velocity, evidence by the variable spacing between the curves, as it propagates onward into material of uniform fracture toughness, $G_{crit} = G_0$.

velocity may be understood as follows. The stress intensity factor $K(z, t)$ is, in general, higher at the retarded parts of the crack than it is at the advanced positions [transient exceptions to this may occur due to the dependency of $K(z, t)$ on the whole prior history of the crack motion]. Since the energy release rate $G(z, t)$ is an increasing function of $K(z, t)$ and a decreasing function of $v(z, t)$ the retarded parts of the crack acquire, in a homogeneous region, higher velocities than the advanced segments. Thus, the retarded parts of the crack approach the advanced positions with higher velocities than those of the advanced parts. This leads to space-time damped oscillatory crack tip motion in the homogeneous region bounding the heterogeneous strip. The oscillatory motion may also be interpreted in terms of constructive-destructive interference of stress intensity waves initiated by encounters of the crack front with asperities and then propagating along the front.

Figure 7 shows crack front positions for the case $v_0/c = 0.5$ and $G_{crit a}/G_{crit 0} = 2$ for both asperities. At this relatively large incoming crack velocity, the asperities break after causing a small retardation in crack front positions. Further crack tip motion

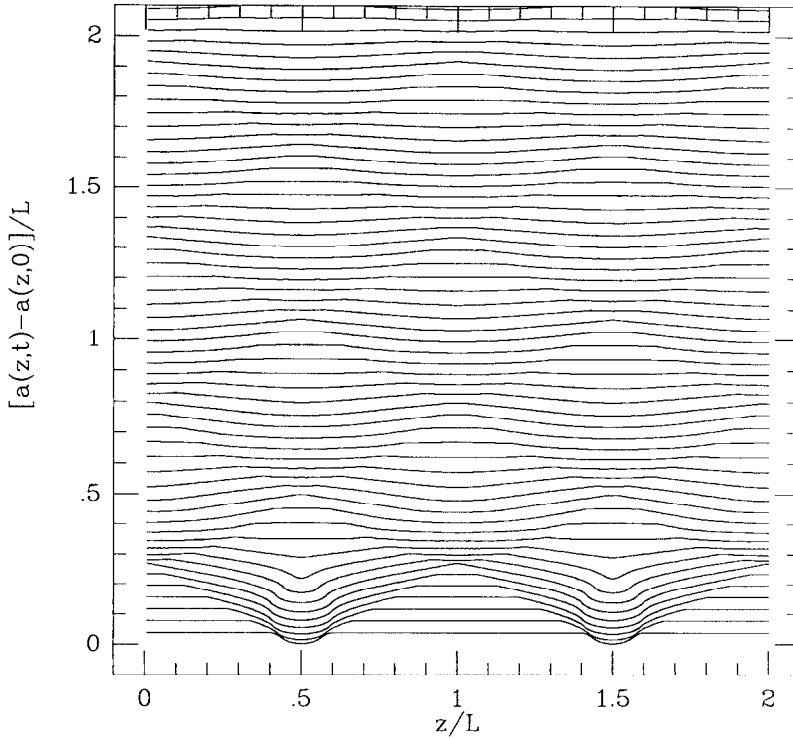


FIG. 7. Positions $a(z, t)$ versus z at successive times, separated by constant intervals, for a crack at incoming speed $v_0 = 0.5c$ hitting an infinite row of asperities with $G_{\text{crit}} = 2G_0$. The crack easily moves through the asperities. Pronounced velocity oscillations occur as it propagates onward into material of uniform fracture toughness, $G_{\text{crit}} = G_0$.

in the homogeneous $G_{\text{crit}0}$ region is marked by damped oscillations. Figure 8 shows calculations for the case $G_{\text{crit}a}/G_{\text{crit}0} = 4$ and other parameters the same as in Fig. 7. Here, as expected, the initial shape deviation caused by the asperities is larger than in Fig. 7. This is followed by oscillatory crack tip motion decaying at a large enough distance from the asperities into a uniformly propagating straight crack. The results shown in Figs 7 and 8 were obtained with $\Delta t = \lambda_{\text{Ny}}/10c$, but resulting plots are not visibly different from those obtained using $\Delta t = \lambda_{\text{Ny}}/5c$ or $\lambda_{\text{Ny}}/15c$.

Since there is mirror symmetry along the z direction relative to $z = 0$ and $z = L$ in Figs 7 and 8, those figures also represent results for crack propagation in a plate of thickness $H = L$ containing a centered asperity, or in a plate of thickness $H = nL$ containing a row of n asperities, where n is some integer.

RANDOM FLUCTUATIONS IN FRACTURE RESISTANCE

Here we describe some results for a case in which the fracture energy $G_{\text{crit}}(x, z)$ is constant at G_0 for $x < 0$, but is a stationary Gaussian random function of position in

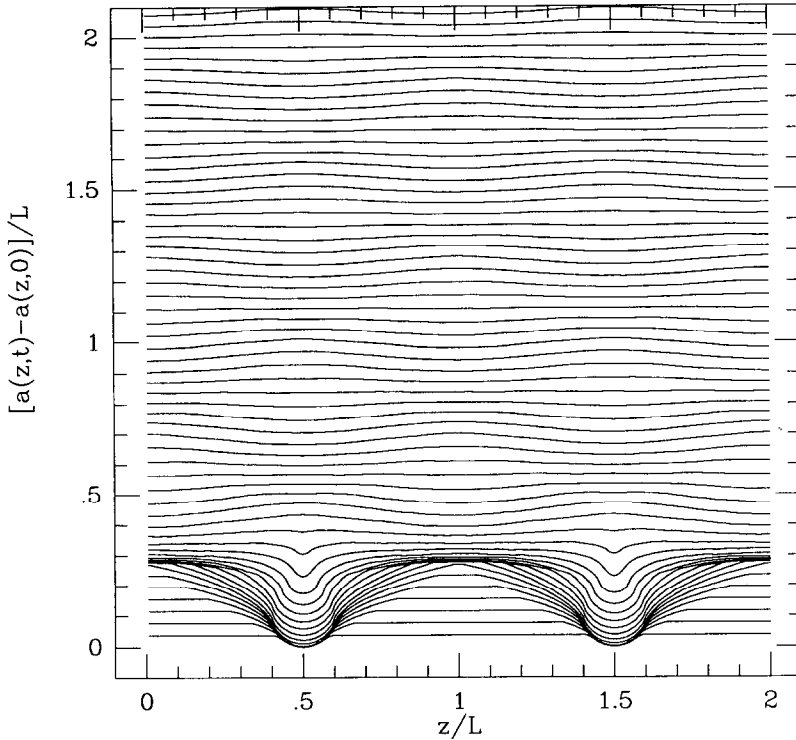


FIG. 8. Positions $a(z, t)$ versus z at successive times, separated by constant intervals, for a crack at incoming speed $v_0 = 0.5c$ hitting an infinite row of asperities with $G_{crit} = 4G_0$. The crack is nearly stopped by the asperities but ultimately moves through, with velocity oscillations occurring as it moves onward through material of uniform fracture toughness, $G_{crit} = G_0$.

the x, z plane, with mean G_0 , for $x > 0$. The random fluctuations from G_0 are assumed to be correlated such that

$$E\{[G_{crit}(x, z) - G_0][G_{crit}(x', z') - G_0]\} = \sigma_{rms}^2 \exp(-\sqrt{(x-x')^2 + (z-z')^2}/b), \quad (54)$$

where E denotes an ensemble expectation, σ_{rms} is the root mean square fluctuation in fracture energy and b is a correlation length. We generate sample functions of G_{crit} over distance λ (the periodic repeat distance for the FFT-based numerical method) in the z direction, and over the total distance to be fractured in the positive x direction, by representing $G_{crit}(x, z)$ as a double Fourier series in x and z . The complex series coefficients are chosen from a random number generator as independent Gaussian variables, each with a variance that corresponds (at least for an infinite number of terms in the series) to the correlation function (54). Each coefficient has identically and independently distributed real and imaginary parts. The sample so generated is replicated periodically in the z direction. Fuller details of the methodology and its application to study the statistics of the associated disordering of the crack tip are intended for presentation in a subsequent paper.

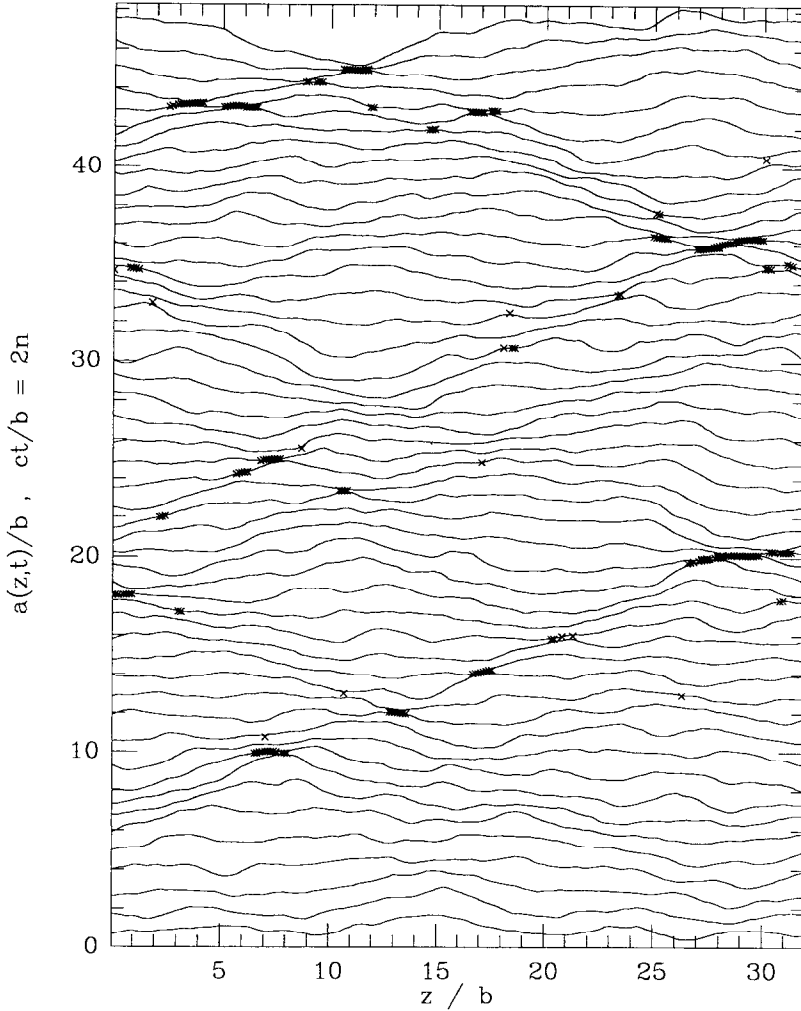


FIG. 9. Positions $a(z, t)$ versus z at successive times, separated by $2.0b/c$, for a crack at incoming speed $v_0 = 0.5c$ which enters into a region $x > 0$ of random variation of fracture energy. The fracture energy $G_{\text{crit}}(x, z)$ in $x > 0$ retains the mean value G_0 , the same as it had in the uniform toughness region $x < 0$, and is chosen from a Gaussian random distribution with root mean square deviation of $\sigma_{\text{rms}} = 0.25G_0$ from that mean, and with an exponentially decaying correlation on the x, z plane with correlation length b . The G_{crit} distribution is truncated at extreme deviations of $\pm 0.75G_0$ from the mean. A sample of $G_{\text{crit}}(x, z)$ generated over a strip of length λ in the z direction is replicated periodically in z for consistency with the FFT-based numerical method. Here $\lambda = 32b$. Symbols \times mark sample points along the crack front at which the propagation velocity has momentarily dropped to zero; their clustering is a dynamic, not a statistical, effect.

Figure 9 shows results for successive positions of the crack front in a case for which $\sigma_{\text{rms}} = 0.25G_0$ and the incoming velocity is $v_0 = 0.5c$. Actually the Gaussian distribution has been truncated in this case so that those rare G_{crit} values (of order 1 sample in 500) which deviate beyond $\pm 0.75G_0$ ($= \pm 3\sigma_{\text{rms}}$) from the mean of G_0 are

re-assigned values of $\pm 0.75G_0$ from the mean. Distances are normalized by b and we have taken $\lambda = 32b$ and $2N = 256$ in the case shown, and used $\Delta t = \lambda_{Ny}/10c = b/40c$. There are many intervals in the history for which some segment of the crack front has momentarily stopped propagating. A symbol \times has been printed at each sample point of crack front position when such an interval begins. Note that the \times symbols tend to cluster over distances that grow to several correlation lengths. This is a dynamical effect triggered by encounter of high G_{crit} locations, particularly when they coincide with locations where the crack is already vulnerable because of a diminished rest value of G (e.g. where the crack front locally protrudes ahead of neighboring segments), and not a statistical effect due to G_{crit} being abnormally high over the entire cluster width. For the scale of the axes shown, wave fronts spread along the moving crack tip at a rate corresponding to lines inclined at $\pm 30^\circ$ with the horizontal axis. It is seen that there is a tendency for later clusters to lie along wave fronts from earlier ones.

The example shown in Fig. 9 represents a mild perturbation of G_{crit} compared to the cases of circular asperities discussed earlier. According to the 2D crack analysis, the representative G_{crit} deviations of $\pm 0.25G_0$ in this case would correspond to $v = (0.50 \pm 0.18)c$. The greatest deviations in the sample, of $+0.75G_0$ (i.e. $G_{crit} = 1.75G_0$), are just sufficient to stop a 2D crack. That happens when $G_{crit} = \sqrt{3}G_0 = 1.732G_0$, a value exceeded with probability of about 1/500. The similarly rare deviations of $-0.75G_0$ (i.e. $G_{crit} = 0.25G_0$) allow the 2D crack a propagation velocity of $0.96c$. The randomly oscillatory velocity history is shown in Fig. 10, where $v(z, t)/c + n$ is plotted as a function of z/b at the specific times given by $ct/b = 8.5n$, where $n = 0, 1, 2, 3, 4, \dots$. This amounts to showing $v(z, t)/c$ within each panel of unit height, displacing the curves for different times from one another. We see that very significant fluctuations in $v(z, t)$ are induced. Occasionally the velocity drops to zero, as already noted, and occasionally very large fractions of c are seen.

DISCUSSION

We have used a model elastodynamic theory, involving a single displacement variable satisfying the scalar wave equation, to study the propagation of a crack along a plane in an unbounded solid. The solution is derived for a crack front whose shape $a(z, t)$ and velocity history $v(z, t)$ is perturbed from that of a straight line moving at uniform speed, and is used to study the effects of spatial variations in fracture energy on perturbing the crack motion. Prolonged oscillatory effects in crack motion are found to follow encounters of the crack front with regions of variable toughness, and these may be explained in terms of interference of stress intensity factor waves radiated along the moving crack front following localized perturbations of crack motion.

The results show remarkable instability features. An initially non-straight crack front which propagates over a plane of strictly uniform fracture energy G_{crit} does asymptotically straighten out. However, our equations have been shown in a related work (PERRIN and RICE, 1994) to imply that small but sustained random fluctuations in G_{crit} over the fracture plane induce a gradually increasing disorder in the crack

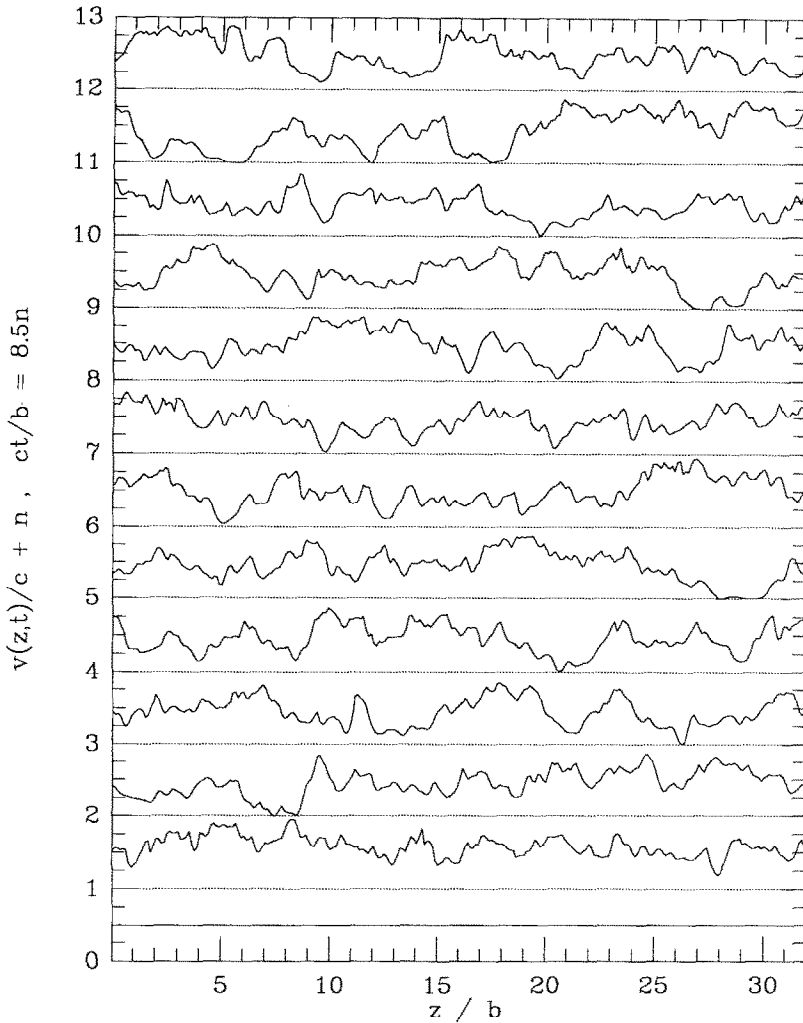


FIG. 10. Same case as Fig. 9. The quantity $v(z,t)/c+n$ is shown as a function of z at specific times chosen as $ct/b = 8.5n$, where $n = 0, 1, 2, 3, 4, \dots, 12$. Thus each horizontal panel of unit height shows the dimensionless velocity v/c at a given time.

front position and motion, so that the straight crack front configuration is, essentially, unstable.

It is clearly important to learn the extent to which such results remain valid in the context of actual elasticity theory, rather than the model theory. Also, while we have rigorously derived 3D results which are valid as first-order perturbations of $v(z, t)$ from uniformity with respect to t and z (what we refer to as the “strictly linearized” formulation), the numerical procedure is based on an extension of those equations which incorporates known exact response to a sudden, finite alteration of $v(z, t)$, and

which exactly replicates the 2D solution for arbitrary crack motion $v = v(t)$. We think this extension is unlikely to result in significant error, but it is important to derive exact results for small perturbations in z about a history $v = v(t)$ of motion that has arbitrary time dependence.

Previous investigators, concerned with 3D elastodynamic shear fracture models for earthquake ruptures, have studied the effects of arrays of asperities (DAS and KOSTROV, 1988) and of random distributions of fracture properties (BOATWRIGHT and QUIN, 1986) on the rupture process. These analyses were done by representing the plane over which fracture may spread, in an unbounded solid, as an array of square cells, each sustaining a shear stress that is uniform but unknown (except initially, before the rupture event begins or waves arrive from it), and by representing the corresponding slip displacements on the fracture as those at cell centers. The stress histories are computed by requiring that stress and slip be related by a constitutive relation, allowing no slip until a threshold “yield stress” is reached and then allowing, in the DAS and KOSTROV (1988) case, slip at an abruptly lower, and constant, dynamic friction strength. BOATWRIGHT and QUIN (1986) allow a continuous degradation of strength from the threshold to the dynamic friction level, with increasing displacement; this slip-weakening feature means that their algorithm should converge, with reduction of cell size, onto a well-defined continuum fracture model of slip-weakening type, with a finite fracture energy. The same is not a feature of the DAS and KOSTROV (1988) procedure which, if it has any continuum limit with cell reduction, would correspond to a surface on which sliding takes place with zero fracture energy; that limitation may possibly be repaired by letting the threshold strength increase with the inverse square root of cell dimension.

These approaches to fracture modeling have an uncertain relation to continuum crack theory. The slip-weakening approach of BOATWRIGHT and QUIN (1986) should correspond to a G_{crit} crack criterion when the weakening zone is small compared to overall rupture size (e.g. RICE, 1980), but numerical accuracy requires that small weakening zone to extend over several cell widths. Their work, as that of DAS and KOSTROV (1988), was restricted by computer limitations such that the grid patch which was allowed to slip had a radius of only about 30–50 cell widths, so that cell size problems could not be fully overcome. Still, the results do show a crack-like rupture propagation over the grid, and BOATWRIGHT and QUIN (1986) report strong non-uniformities in rupture velocity, similar to our results here, when moderate random heterogeneity is introduced in their distributions of initial stress and critical breaking stress. DAS and KOSTROV (1988) examine the effects of an array of square asperities on the distant wavefield radiated by the rupture. They expected, and found, that local peaks in the radiated waveform correspond to the rupture of asperities, but they report also that “additional peaks not related to the failure of any asperity were found... [and that]... no simple correlation was found between the number of asperities fracturing and the number of peaks” (DAS and KOSTROV, 1988, p. 8049), although those peaks directly attributable to asperity failures were the most prominent on the waveform. While Das and Kostrov do not show the history of rupture velocity or successive positions of the rupture front, it seems that the type of oscillatory crack motion that we document here, from the interference effects of stress intensity waves radiated by earlier asperity failures, could be the basis for their observations. For

natural earthquakes the lesson may be that not all the source complexity inferred from recorded waveforms is to be regarded as corresponding to material or geometric heterogeneity along the rupture surface.

The effects that we have reported in this paper may also be relevant to a puzzle of long duration in the tensile cracking of brittle solids such as glass and PMMA, the phenomenology of which is summarized by KNAUSS and RAVI-CHANDAR (1985). In such materials, a fracture surface which is optically smooth and planar at low speeds develops pronounced roughness, sometimes accompanied by macroscale crack branching, as speed increases. Careful recent measurements by GROSS *et al.* (1993), extending techniques reported by FINEBERG *et al.* (1992), show that this roughness transition takes place at speed $v = 0.42\text{--}0.49c_R$ for soda lime glass and $v = 0.42\text{--}0.47c_R$ for PMMA. Here c_R is the Rayleigh speed; $c_R \approx 0.92c_s$ for Poisson ratio of 0.3, as used in the subsequent discussion, and c_s is the shear wave speed; c_R is the limiting speed, analogous to c of the model theory, for a tensile crack which propagates in a plane.

Previous attempts to explain this roughening transition have led to significantly larger predicted transition speeds. Such began with YOFFE (1951) observing that the hoop tensile stress at a given small radius from the crack tip attains a maximum on the plane prolonging the crack plane for $v < 0.60c_R$, but that the maximum shifts to about 60° from that plane at higher speeds. The same transition speed $v \approx 0.60c_R$ was recently shown by GAO (1993) to be the speed above which G for a direction of crack growth that does not prolong the crack plane is greater than for one which does. GAO (1993) also presents a significant result for 2D dynamic cracking along a slightly non-straight crack path, in the presence of loading by what would be, in the straight-cracked solid, a locally uniform crack-parallel tensile stress T which acts in addition to the $r^{-1/2}$ singular stress field. It has been shown (COTTERELL and RICE, 1980) that $T < 0$ is necessary for configurational stability of a straight tensile crack path under quasi-static conditions, assuming that the crack grows under pure tensile mode conditions at its tip. KNAUSS and RAVI-CHANDAR (1985) show from experimental results that the same criterion holds good in the early stages of dynamic crack growth. GAO's (1993) result, the implications of which he does not discuss, is that the same $T < 0$ which allows an initially straight crack path to exist at low speeds destabilizes that straight path when $v > 0.75c_R$; any small deviations from straightness then get amplified, according to Gao's dynamic linearized stability analysis. Such amplification of small initial deviations from straightness is a description of roughening, and ultimately macro-branching, which is supported by the observations of KNAUSS and RAVI-CHANDAR (1985). Thus it would seem that $v = 0.75c_R$ is a definitive upper limit to the possible speed of planar crack growth in an isotropic brittle solid, although factors compatible with non-planar growth are identifiable at $v > 0.60c_R$.

Why, then, does the roughness transition occur for $v \approx 0.45c_R$? Our results here suggest a possible answer which has some observational support: the experimentally reported crack speeds at the roughness transition are averages over finite space and time intervals. If our results carry over to tensile cracks, then it must be recognized that inevitable small fluctuations in fracture energy of the material drive a disordering of the crack front, ultimately showing as a highly variable local velocity, perhaps like in Fig. 10. In order for roughness to appear on the previously mirror-like fracture

surface, it is necessary only that the fastest moving parts of the crack front reach the high speeds of the Yoffe–Gao range ($0.60\text{--}0.75c_R$) and trigger micro-branching instabilities, which can happen when the average speed is much lower. It is unknown at this point if this conjectured oscillation mechanism could explain the observed speeds of order $0.45c_R$, but there is definitive experimental evidence that crack velocities in such brittle materials do indeed become severely oscillatory. That is a pronounced effect during the stage of propagation with a roughened surface (KNAUSS and RAVI-CHANDAR, 1985; FINEBERG *et al.*, 1992), and the results of FINEBERG *et al.* (1992) show also that the velocity has already become oscillatory, in consistency with expectations from our work, well before the roughness transition, when the fracture surface is still optically smooth and planar.

Another perspective on the roughness transition follows ESHELBY (1970) who posed the question of how large must v be so that, by decelerating, there is enough energy available to supply to two crack surfaces the same G as was being supplied to one. The least v before deceleration corresponds to $v = 0^+$ just afterwards, and the simplest branched configuration to analyse, and quite plausibly the one which maximizes energy flow after branching, is the idealized limit case when the branches subtend a vanishing angle and both prolong the original crack plane. Thus the minimum v is that for which the “rest” value of G , i.e. G^* for the 2D crack, is twice that for propagation at v . From the v dependence in (9) and (33a), which is of the same structure as for ESHELBY’S (1969a, b) anti-plane shear analysis if $c = c_s$, ESHELBY (1970) reported $v = 0.60c_s \approx 0.65c_R$ as the minimum v which could allow branching or surface roughening. This value is sometimes reported in the literature. However, ESHELBY (1970) wrote before the FREUND (1972a) solution for unsteady crack motion in the tensile mode became available and, writing the tensile analog of equation (9) as $G = g(v)G^*$, FREUND (1972a, pp. 138–139) plots the function $g(v)$ and notes that the corresponding speed, solving $g(v) = 1/2$, is $v \approx 0.45c_R$. Thus, although the Yoffe–Gao explanations of how non-planar roughness features can form and grow require greater speeds of $0.60\text{--}0.75c_R$, the Eshelby–Freund minimum speed of $0.45c_R$ for the requisite energy to be supplied for roughening is in good agreement with the speeds at roughness onset found experimentally (GROSS *et al.*, 1993).

ACKNOWLEDGEMENTS

These studies were supported by the Office of Naval Research, Mechanics Division, under grant N00014-90-J-1379 to Harvard University. Partial support in the early stages of the study was provided by the U.S. Geological Survey, Earthquake Hazards Reduction Program, under grants 14-08-001-G-1788 and G-2276. We are grateful to Gilles Perrin for discussions and to John Morrissey for discussions and assistance in the calculations for Figs 9 and 10.

REFERENCES

- ABRAMOWITZ, M. and STEGUN, A. (1972) *Handbook of Mathematical Functions*. Dover, New York.
- AKI, K. and RICHARDS, P. G. (1980) *Quantitative Seismology: Theory and Methods*. W. H. Freeman and Company, San Francisco.

- BEN-ZION, Y. (1989) The response of two joined quarter spaces to SH line sources located at the material discontinuity interface. *Geophys. J. Int.* **98**, 213–222.
- BOATWRIGHT, J. and QUIN, H. (1986) The seismic radiation from a 3-D dynamic model of a complex rupture process. Part I: confined ruptures. *Earthquake Source Mechanics* (ed. S. DAS, J. BOATWRIGHT and C. H. SCHOLZ), pp. 97–109. American Geophysical Union, Washington, DC.
- CAGNIARD, L. (1939) *Reflexion et Refraction es Ondes Seismiques Progressives*. Gauthier-Villiers, Paris.
- CAGNIARD, L. (1962) *Reflection and Refraction of Progressive Seismic Waves*, translated and revised by E. A. FLINN and C. H. DIX. McGraw-Hill, New York.
- COTTERELL, B. and RICE, J. R. (1980). Slightly curved or kinked cracks. *Int. J. Fract.* **16**, 155–169.
- DAS, S. and KOSTROV, B. V. (1988) An investigation of the complexity of the earthquake source time function using dynamic faulting models. *J. Geophys. Res.* **93**, 8035–8050.
- DE HOOP, A. T. (1961) A modification of Cagniard's method for solving seismic pulse problems. *Appl. Sci. Res.* **B8**, 349–356.
- DMOWSKA, R. and RICE, J. R. (1986) Fracture theory and its seismological application. *Continuum Theories in Solid Earth Physics* (Vol. 3 of series "Physics and Evolution of the Earth's Interior"; ed. R. TEISSEYRE), pp. 187–255. Elsevier and Polish Scientific Publishers.
- ESHELBY, J. D. (1969a) The elastic field of a crack extending non-uniformly under general anti-plane loading. *J. Mech. Phys. Solids* **17**, 177.
- ESHELBY, J. D. (1969b) The starting of a crack. *Physics of Strength and Plasticity* (ed. A. S. ARGON), pp. 263–275. The MIT Press, Cambridge and London.
- ESHELBY, J. D. (1970) Energy relations and the energy-momentum tensor in continuum mechanics. *Inelastic Behavior of Solids* (ed. M. F. KANNINEN, W. F. ADLER, A. R. ROSENFELD and R. I. JAFFE), pp. 77–115. McGraw-Hill, New York.
- FARES, N. (1989) Crack fronts trapped by arrays of obstacles: numerical solutions based on surface integral representations. *J. Appl. Mech.* **56**, 837–843.
- FINEBERG, J., GROSS, S. P., MARDER, M. and SWINNEY, H. L. (1992) An instability in the propagation of fast cracks. *Phys. Rev. B* **45**, 5146–5154.
- FOSSUM, A. F. and FREUND, L. B. (1975) Non-uniformly moving shear crack model of shallow focus earthquake mechanics. *J. Geophys. Res.* **80**, 3343–3347.
- FREUND, L. B. (1972a) Crack propagation in an elastic solid subject to general loading—I. Constant rate of extension.—II. Non-uniform rate of extension. *J. Mech. Phys. Solids* **20**, 129–140, 141–152.
- FREUND, L. B. (1972b) Energy flux into the tip of an extending crack in an elastic solid. *J. Elasticity* **2**, 341–349.
- GAO, H. (1993) Surface roughening and branching instabilities in dynamic fracture. *J. Mech. Phys. Solids* **41**, 457–486.
- GAO, H. and RICE, J. R. (1989) A first-order perturbation analysis of crack trapping by arrays of obstacles. *J. Appl. Mech.* **56**, 828–836.
- GROSS, S. P., FINEBERG, J., MARDER, M., MCCORMICK, W. D. and SWINNEY, H. L. (1993) Acoustic emissions from rapidly moving cracks. *Phys. Rev. Lett.*, **71**, 3162–3165.
- KNAUSS, W. G. and RAVI-CHANDAR, K. (1985) Some basic problems in stress wave dominated fracture. *Int. J. Fract.* **27**, 127–143.
- KOSTROV, B. V. (1966) Unsteady propagation of longitudinal shear cracks. *Appl. Math. Mech.* (English translation of *Prikl. Mat. i Mek.*) **30**, 1241–1248.
- KOSTROV, B. V. (1975) On the crack propagation with variable velocity. *Int. J. Fract.* **11**, 47–56.
- PERRIN, G. and RICE, J. R. (1994) Disorder of a dynamic planar crack front in a model elastic medium of randomly variable toughness. *J. Mech. Phys. Solids*, in press.
- RICE, J. R. (1980) The mechanics of earthquake rupture. *Physics of the Earth's Interior* (Proc. International School of Physics 'Enrico Fermi', Course 78, 1979; ed. A. M. DZIEWONSKI and E. BOSCHI), pp. 555–649. Italian Physical Society and North-Holland Publ. Co.

RICE, J. R. (1985) First order variation in elastic fields due to variation in location of a planar crack front. *J. Appl. Mech.* **52**, 571–579.

RICE, J. R. (1989) Weight function theory for three-dimensional elastic crack analysis. *Fracture Mechanics: Perspective and Directions* (Twentieth Symposium), Special Technical Publication 1020 (ed. R. P. WEI and R. P. GANGLOFF), pp. 29–57. ASTM, Philadelphia.

YOFFE, E. H. (1951) The moving Griffith crack. *Phil. Mag.* **42**, 739–750.

APPENDIX A: DERIVATION OF SPACE-TIME FORM OF SOLUTION FOR ϕ FROM TRANSFORM SOLUTION

To derive (27) from (26), let us note that if $f(z, -\infty) = 0$ we may write

$$f(z, t) = \int_{-\infty}^{+\infty} \int_{-\infty}^{+\infty} H(t-t') \delta_D(z-z') \frac{\partial f(z', t')}{\partial t'} dt' dz', \tag{A1}$$

where H is the Heaviside unit step function and δ_D is the Dirac unit impulse function. Hence to solve for $\phi(x, y, z, t)$ for a general $f(z, t)$ we can superpose, by integration over z' and t' with weighting $\partial f(z', t')/\partial t'$, the solution $\phi(x, y, z, t; z', t')$ corresponding to $f(z, t) = H(t-t')\delta_D(z-z')$. The Fourier transform of $H(t-t')\delta_D(z-z')$ is

$$F(k, \omega) = (1/i\omega) \exp[-i\omega t' + ikz']. \tag{A2}$$

We insert this $F(k, \omega)$ into (26) to get the kernel solution for the superposition,

$$\phi(x, y, z, t; z', t') = \frac{A}{2\pi i} \int_{-\infty}^{+\infty} \int_{-\infty}^{+\infty} \exp[i\omega(t-\delta) - ikz_1 - q(k, \omega)r] \frac{d\omega}{\omega} dk, \tag{A3}$$

where

$$\delta = t' + v_0(x - v_0 t)/\alpha_0^2 c^2, \quad z_1 = z - z', \quad A = \frac{\sin(\theta/2)}{\sqrt{2\pi r}} \frac{K_0}{M\alpha_0} \frac{1}{2\pi} \quad \text{and} \quad q(k, \omega)$$

is defined by (20).

This solution for $\phi(x, y, z, t; z', t')$ is in a form amenable for a Cagniard-de Hoop inversion. The first step in the Cagniard-de Hoop method is to write an integral solution in the Laplace domain, the integration corresponding to an inverse Fourier transform. The integration path is then deformed in a complex ray parameter domain until the solution resembles a forward Laplace transform, from which the time domain solution can be identified. The complex domain manipulation is, in effect, a cancellation process between the inverse Laplace and Fourier transforms. Thus, making the substitution $\omega = -is$, the above solution can be written

$$\phi(x, y, z, t; z', t') = \frac{1}{2\pi i} \int_{-i\infty}^{+i\infty} \exp(st) \Phi(s; \delta, z_1, r, A) ds, \tag{A4}$$

where

$$\Phi(s; \delta, z_1, r, A) = \frac{A}{s} \int_{-\infty}^{+\infty} \exp[-s\delta - ikz_1 - q(k, -is)r] dk. \tag{A5}$$

Treating δ, z_1, r and A as given parameters (note that three of them are actually functions of time, in that they depend on $x - v_0 t$), we can regard $\phi(x, y, z, t; z', t')$ as the function of t of which the Laplace transform is $\Phi(s; \delta, z_1, r, A)$. Writing $k = -isp$, with s regarded henceforth as a real positive number, we have

$$\Phi(s; \delta, z_1, r, A) = -iA \exp(-s\delta) \int_{-i\infty}^{i\infty} \exp\{-s[pz_1 + \eta(p)r/\alpha_0]\} dp, \tag{A6}$$

where $\eta(p) = \sqrt{(\alpha_0 c)^{-2} - p^2}$ is descended from the expression for $q(k, \omega)$ given in (20). Following the discussion of the branch cuts of $q(k, \omega)$, the positive square root is implied for $\eta(p)$ when p lies on the imaginary axis.

The integrand in (A4) can be written as $\text{Int}(p) = E(p) + O(p)$, where $E(p)$ and $O(p)$ are even and odd functions of p , respectively. Since the range of integration in (A6) is symmetric in p we have

$$\int_{-i\infty}^{i\infty} \text{Int}(p) dp = 2 \int_0^{i\infty} E(p) dp = 2 \int_0^{i\infty} \text{Re}[\text{Int}(p)] dp = 2i \text{Im} \int_0^{i\infty} \text{Int}(p) dp \quad (\text{A7})$$

or explicitly

$$\Phi(s; \delta, z_1, r, A) = 2A \exp(-s\delta) \text{Im} \int_0^{i\infty} \exp\{-s[pz_1 + \eta(p)r/\alpha_0]\} dp. \quad (\text{A8})$$

Changing now the integration variable from the ‘‘ray parameter’’ p to the ‘‘travel time’’ τ along the ray, by defining $\tau = pz_1 + \eta(p)r/\alpha_0$ as the coefficient of s in the integrand above, we write

$$\Phi(s; \delta, z_1, r, A) = 2A \exp(-s\delta) \text{Im} \int_{p(\tau)=0}^{p(\tau)=i\infty} \exp(-s\tau) [dp(\tau)/d\tau] d\tau. \quad (\text{A9})$$

Using $\eta(p)$ in the expression for τ above, p can be expressed in terms of τ to give the functions $p(\tau)$ and $dp(\tau)/d\tau$ [they can also be obtained from results of BEN-ZION (1989) by variable substitutions]. Using the fact that the positive square root is implied in $\eta(p)$ when p lies along the imaginary axis, $p = 0$ corresponds to $\tau = r/\alpha_0^2 c$. If we now let τ increase monotonically through real values from $\tau = r/\alpha_0^2 c$ to $\tau = \infty$, the path followed by p which terminates at infinity in the region $\text{Im}(p) > 0$ is

$$p(\tau) = \frac{z_1 \tau}{R^2} - \frac{z_1 r}{|z_1| \alpha_0 R^2} \sqrt{\frac{R^2}{\alpha_0^2 c^2} - \tau^2}, \quad \frac{r}{\alpha_0^2 c} < \tau < \frac{R}{\alpha_0 c}, \quad \text{and}$$

$$p(\tau) = \frac{z_1 \tau}{R^2} + i \frac{r}{\alpha_0 R^2} \sqrt{\tau^2 - \frac{R^2}{\alpha_0^2 c^2}}, \quad \frac{R}{\alpha_0 c} < \tau < \infty, \quad (\text{A10})$$

where $R = \sqrt{z_1^2 + r^2/\alpha_0^2}$. Note that the range over which the first expression for $p(\tau)$ applies shrinks to zero when $z_1 = 0$. This path is deformed away from the imaginary p axis, but crosses no singularities and leaves the integral invariant. [See Fig. 2 of BEN-ZION (1989) for a sketch of such a path in his analysis of a wave problem that involves a function $\eta(p)$ of similar structure.] Since the first expression for $p(\tau)$ gives real $dp(\tau)/d\tau$ over the range of τ for the expression, that range of τ will not contribute to (A9). Rather, we have the entire contribution from the range of the second expression, over which

$$\frac{dp(\tau)}{d\tau} = \frac{z_1}{R^2} + i \left(\frac{r\tau}{\alpha_0 R^2} \right) / \sqrt{\tau^2 - \frac{R^2}{\alpha_0^2 c^2}}, \quad \frac{R}{\alpha_0 c} < \tau < \infty. \quad (\text{A11})$$

Upon substitution in (A9), we retain only the imaginary part, and thus obtain

$$\Phi(s; \delta, z_1, r, A) = 2A \int_{R/\alpha_0 c}^{\infty} \exp[-s(\tau + \delta)] \left[\left(\frac{r\tau}{\alpha_0 R^2} \right) / \sqrt{\tau^2 - \frac{R^2}{\alpha_0^2 c^2}} \right] d\tau. \quad (\text{A12})$$

Now, making the substitution $\tau = t - \delta$ for the variable of integration, this becomes

$$\Phi(s; \delta, z_1, r, A) = \int_{\delta + R/\alpha_0 c}^{\infty} \exp(-st) \left[\left(\frac{2Ar(t - \delta)}{\alpha_0 R^2} \right) / \sqrt{(t - \delta)^2 - \frac{R^2}{\alpha_0^2 c^2}} \right] dt \quad (\text{A13})$$

which can evidently be interpreted as the Laplace transform of the function of t given in the

square brackets times the Heaviside unit step $H(t - \delta - R/\alpha_0 c)$. Remembering that $\phi(x, y, z, t; z', t')$ is the function of t whose Laplace transform is $\Phi(s; \delta, z_1, r, A)$, when δ, z_1, r, A are regarded as given parameters, we find that the desired solution is

$$\phi(x, y, z, t; z', t') = 2AH(t - \delta - R/\alpha_0 c)[(t - \delta)^2 - (R/\alpha_0 c)^2]^{-1/2} r(t - \delta)/(\alpha_0 R^2) \quad (A14)$$

where all of A, r, R, δ and z_1 have been defined above.

Rearranging terms with the aid of rather elaborate algebraic manipulations, we write the solution in the more explicit form

$$\phi(x, y, z, t; z', t') = \sqrt{\frac{r}{2\pi}} \frac{K_0 \sin(\theta/2)}{M\alpha_0 \pi} \frac{c(t-t') - v_0(x-v_0 t)/\alpha_0^2 c}{(z-z')^2 + y^2 + (x-v_0 t)^2/\alpha_0^2} \cdot \frac{H[c(t-t') - \sqrt{(z-z')^2 + y^2 + (x-v_0 t)^2}]}{\sqrt{c^2(t-t')^2 - (z-z')^2 - y^2 - (x-v_0 t)^2}} \quad (A15)$$

As remarked at the start of this Appendix, to obtain the solution for $\phi(x, y, z, t)$ for an arbitrary $f(z, t)$, this solution for $\phi(x, y, z, t; z', t')$ is to be weighted with $\partial f(z', t')/\partial t'$ and integrated over the variables z' and t' . Such is the origin of the general space-time solution given in the text as (27).

APPENDIX B: ALTERNATIVE FORMS FOR THE HISTORY INTEGRAL $I(z, t)$

The expressions for stress intensity factor and energy release rate derived in the paper contain the integral

$$I(z, t) = \frac{1}{2\pi} PV \int_{-\infty}^{\infty} \int_{-\infty}^{t-|z-z'|/\alpha_0 c} \frac{c(t-t')[v(z', t') - v(z, t')]}{(z-z')^2 \sqrt{\alpha_0^2 c^2(t-t')^2 - (z-z')^2}} dt' dz' \quad (B1)$$

where $v(z, t) = \partial a(z, t)/\partial t$. Considering the domain of integration (Fig. B1) and changing the order and limits of the integrals in (B1) we have

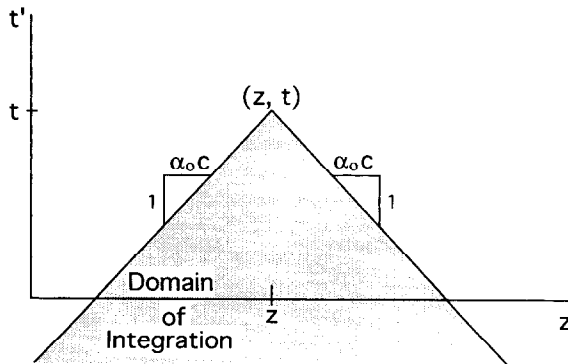


FIG. B1. Domain of integration in (B1); only points within the shaded region influence the crack response at (z, t) .

$$I(z, t) = \frac{1}{2\pi} PV \int_{-\infty}^t \int_{z-\alpha_0 c(t-t')}^{z+\alpha_0 c(t-t')} \frac{c(t-t')[v(z', t') - v(z, t')]}{(z-z')^2 \sqrt{\alpha_0^2 c^2 (t-t')^2 - (z-z')^2}} dz' dt'. \tag{B2}$$

Referring to Fig. B2 we note that the recurring term

$$\alpha_0^2 c^2 (t-t')^2 - (z-z')^2 \equiv [c(t-t')]^2 - [v_0(t-t')]^2 - (z-z')^2 \tag{B3}$$

corresponds at first order to $[c(t-t')]^2 - [a(z, t) - a(z', t')]^2 - (z-z')^2$ which has a clear interpretation in terms of travel times, t' being the moment of release of a signal at z' along the front which arrives at z along the (then advanced) crack front at time t . A portion of the integrand in $I(z, t)$ can be written as

$$\begin{aligned} \frac{c(t-t')}{(z-z')^2 \sqrt{\alpha_0^2 c^2 (t-t')^2 - (z-z')^2}} &= - \frac{\partial}{\partial z'} \left[\frac{\sqrt{\alpha_0^2 c^2 (t-t')^2 - (z-z')^2}}{\alpha_0^2 c (t-t') (z-z')} \right] \\ &= - \frac{\partial}{\partial t'} \left[\frac{\sqrt{\alpha_0^2 c^2 (t-t')^2 - (z-z')^2}}{\alpha_0^2 c (z-z')^2} \right]. \end{aligned} \tag{B4}$$

Using the first version of (B4) and integrating by parts in (B2) leads to

$$I(z, t) = \frac{1}{2\pi} PV \int_{-\infty}^t \int_{z-\alpha_0 c(t-t')}^{z+\alpha_0 c(t-t')} \frac{\sqrt{1 - [(z'-z)^2 / \alpha_0^2 c^2 (t-t')^2]}}{\alpha_0 (z'-z)} \frac{\partial v(z', t')}{\partial z'} dz' dt', \tag{B5a}$$

whereas recognizing that $-\partial/\partial z'$ can be replaced by $\partial/\partial z$ in (B4) gives

$$I(z, t) = \frac{1}{2\pi} PV \frac{\partial}{\partial z} \int_{-\infty}^t \int_{z-\alpha_0 c(t-t')}^{z+\alpha_0 c(t-t')} \sqrt{1 - \frac{(z'-z)^2}{\alpha_0^2 c^2 (t-t')^2}} \frac{v(z', t') - v(z, t')}{\alpha_0 (z'-z)} dz' dt'. \tag{B5b}$$

Similarly, based on the second form of (B4) with $-\partial/\partial t'$ replaced by $\partial/\partial t$,

$$I(z, t) = \frac{1}{2\pi} PV \frac{\partial}{\partial t} \int_{-\infty}^x \int_{-\infty}^{t-|z-z'|/\alpha_0 c} \sqrt{\alpha_0^2 c^2 (t-t')^2 - (z-z')^2} \frac{v(z', t') - v(z, t')}{\alpha_0^2 c (z-z')^2} dt' dz', \tag{B6a}$$

and integration of that result by parts after using $v(z, t) = \partial a(z, t)/\partial t$ leads to

$$I(z, t) = \frac{1}{2\pi} PV \frac{\partial}{\partial t} \int_{-\infty}^x \int_{-\infty}^{t-|z-z'|/\alpha_0 c} \frac{c(t-t')[a(z', t') - a(z, t')]}{(z-z')^2 \sqrt{\alpha_0^2 c^2 (t-t')^2 - (z-z')^2}} dt' dz'. \tag{B6b}$$

Finally, we observe [see (B3) and Fig. B2] that the upper integration limit on t' is the latest time t' for which a signal launched at the crack front at (z', t') will reach (z, t) along the then

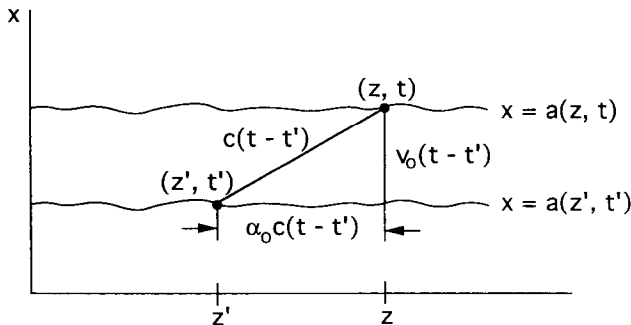


FIG. B2. Geometrical relationships between wave speed c , crack speed v_0 and speed of propagation $\alpha_0 c$ along the crack front.

advanced front. That value of t' is the first order perturbation representation of the time $\tau = \tau(z, z', t)$ satisfying

$$c^2(t - \tau)^2 = [a(z, t) - a(z', \tau)]^2 + (z - z')^2, \tag{B7}$$

and thus we may write

$$I(z, t) = \frac{1}{2\pi} PV \int_{-\infty}^{\infty} \int_{-\infty}^{\tau(z, z', t)} \frac{c(t - t') [v(z', t') - v(z, t')]}{(z - z')^2 \sqrt{c^2(t - t')^2 - [a(z, t) - a(z', t')]^2 - (z - z')^2}} dt' dz'. \tag{B8}$$

Expression (B8) for $I(z, t)$ contains no reference to a uniform velocity v_0 about which a perturbation is made, and it might possibly be valid for arbitrarily large variations of $v(z, t)$ with t , as long as $|\partial a(z, t) / \partial z| \ll 1$ (i.e. for small deviations from straightness but arbitrary deviations from a uniform propagation velocity). We caution that such has not been proven.